Pis'ma v ZhETF, vol. 94, iss. 8, pp. 704 – 709

Spin-related phenomena in InAs/GaSb quantum wells

A. Zakharova[+], *I. Semenikhin*[+], *K. A. Chao*[*×]

[+] *Institute of Physics and Technology RAS, 117218 Moscow, Russia*

[*] *Department of Physics, Lund University, S-22362 Lund, Sweden*

[×] *Department of Physics, Chemistry and Biology, Linköping University, S-58183 Linköping, Sweden*

Submitted 14 July 2011

Resubmitted 13 September 2011

We have studied theoretically the influence of symmetry breaking mechanisms: structural inversion asymmetry, bulk inversion asymmetry, relativistic and non-relativistic interface Hamiltonian and warping on spin split of levels ΔE and optical absorption of linearly polarized light in asymmetrical quantum wells made from zinc-blende materials grown on [001] direction. The AlSb/InAs/GaSb/AlSb broken-gap quantum wells with hybridized electron-hole states sandwiched by the AlSb barriers have been considered. We have obtained substantial contributions of these effects into the absolute values of spin split of electron and hole states and spin-flip optical transitions for the initial state in-plane wave vectors along low symmetry directions such as [12].

Since the pioneering work by M. Altarelli [2] on the energy band structures of InAs/GaSb superlatticies, the broken-gap heterostructures have been studied extensively experimentally [3–7] and theoretically [1, 8–15]. Such structures are very interesting from the point of view of fabrication different electronic devices especially light emitted diodes and lasers [4, 10]. However, they can be used also for quantum computing because of large spin split of levels in the InAs/GaSb quantum wells sandwiched by the two AlSb barriers originated from the Rashba and Dresselhaus effects [15, 16]. In these quantum wells, the InAs conduction band edge is below the GaSb valence band edge even at zero external bias. For this reason, the electron states in the InAs layer of the quantum well can hybridize with the light hole and heavy hole states in the GaSb layer. These hybridization is especially strong when the lowest electron-like level $1e$ at the zone center (in-plane wave vector $\mathbf{k}_{\|}$=0) is lower than the highest heavy hole level $1hh$. In this case, the $1e$ and $1hh$ states anticross with the in-plane wave vector increasing and the hybridization gap appears in the in-plane dispersion [2, 6, 7, 9, 10, 12]. The hybridization mixes the electron and hole states and influences the optical matrix elements for the transitions between different subbands [9, 10]. Different symmetry breaking mechanisms such as bulk inversion asymmetry (BIA), structural inversion asymmetry (SIA), relativistic and non-relativistic interface Hamiltonian (IH) with spin-orbit interaction also influences the energy level positions, wave functions and, hence optical matrix elements and absorption coefficients [1, 9, 13–15]. They give rise to a considerable spin split of subbands and intensity of spin-flip inter-subband infrared transitions for different directions of initial state in-plane wave vectors. The aim of this paper is to investigate these effects for different values and directions of electron or hole state in-plane wave vector including low symmetry directions.

We use the Burt–Foreman envelope function theory [17, 18] and eight-band Hamiltonian which takes into account the conduction band states, light hole states, heavy hole states and the states in the split-off band precisely. The other remote band are treated with perturbation theory. Hamiltonian includes the strain-dependent terms resultant from the lattice-mismatch, BIA and IH. The warping, which also creates the subband anisotropy especially for the valence band states, appears in the model due to the inequality of second and third Luttinger parameters. The energy level positions, spin spit of two dimensional electron and hole states and optical matrix elements are investigated with account of the self-consistent potential created by carriers in the InAs/GaSb quantum well and contact layers. We have found a substantial enlarge of spin split of levels due to BIA and IH and the intensity of spin-flip optical transitions for the light polarized along the [001] growth direction due to combined effect of warping and symmetry breaking.

We will consider the InAs/GaSb quantum wells grown on InAs along the [001] crystal direction which we will define as the z-axis. The x-axis is along the [10] direction in the plane of the quantum well, and the y-axis is along the [01] direction. The eight-band Burt–Foreman $\mathbf{k}\cdot\mathbf{p}$ Hamiltonian can written using a set a basis functions near the Γ point

$$S\uparrow,\ X\uparrow,\ Y\uparrow,\ Z\uparrow,\ S\downarrow,\ X\downarrow,\ Y\downarrow,\ Z\downarrow\ . \qquad (1)$$

The Hamiltonian is given by

$$\hat{H} = \begin{pmatrix} \hat{H}_4 & 0 \\ 0 & \hat{H}_4 \end{pmatrix} + \hat{H}_{so} + \hat{H}_{\epsilon} + \hat{H}_{\epsilon k} + \hat{H}_B + \hat{H}_k. \quad (2)$$

The 4×4 matrix $\hat{H}_4$ depends on the conduction band edge E_C, the valence band edge E_V, the momentum operators, the interband momentum matrix elements $P(z)$, and the modified Luttinger parameters. The second term $\hat{H}_{so}$ and the third term $\hat{H}_{\epsilon}$, which are independent of the momentum operators, describe, respectively, the effect of spin-orbit interaction and the lattice-mismatched strain on energy levels and wave functions. These terms are listed in Ref. [12]. The next two terms $\hat{H}_{\epsilon k}$ and $\hat{H}_B$ appear due to BIA. The term $\hat{H}_k$ is the IH, which has relativistic and non-relativistic part. The operators in $\hat{H}_{\epsilon k}$ are proportional to the strain tensor components ϵ_{ij} and the momentum operator components $\hat{k}_l$. The operator $\hat{H}_B$ depends on Kane's B parameters. The BIA and IH terms are listed in Ref. [1]. The IH is nonzero only at the interfaces and influences only the boundary conditions at the heterojunctions. However, the BIA terms effect not only the boundary conditions but also the optical transition operator giving rise to a specific interface contribution to the optical matrix elements [1].

The energy level positions and wave functions can be found from the Schrödinger equation

$$\hat{H}\Psi = E\Psi\,, \quad (3)$$

where Ψ is the multi-component envelope function and E the energy. We use the basis expansion method [19] to solve the Schrödinger equation self-consistently with the Poisson equation. Using the obtained energy levels and wave functions, we will find the spin split of levels and optical matrix elements for the transitions from the initial states having the in-plane wave vectors along different directions such as [10] and [12].

The probability of optical transition between the state l in one subband and the state k in the other subband cause by polarized light with $\mathbf{e}$ as the unit vector of polarization can be defined in terms of the velocity operator

$$\hat{\mathbf{v}} = \frac{1}{\hbar}\frac{\partial \hat{H}}{\partial \hat{\mathbf{k}}}\,. \quad (4)$$

Then the optical transition operator $\mathbf{e}\cdot\hat{\mathbf{v}}$ determines the optical matrix element

$$M = (2m)^{1/2}\,\langle \Psi_{\mathbf{k}}|\mathbf{e}\cdot\hat{\mathbf{v}}|\Psi_{\mathbf{l}}\rangle, \quad (5)$$

where m is a free electron mass. If in the operator $\hat{H}$ in Eq. (4) we keep only the terms proportional to the interband momentum matrix element $P(z)$, our Eq. (5) reduces to the commonly used equation for the optical matrix element

$$M = \left(\frac{2}{m}\right)^{1/2}\langle \psi_k|\mathbf{e}\cdot\hat{\mathbf{p}}|\psi_l\rangle, \quad (6)$$

where ψ_k and ψ_l are the Bloch functions, and $\hat{\mathbf{p}}$ the momentum operator. We should point out that in the expression Eq. (6), the effect of remote bands is neglected in the optical transition operator. Consequently, in this operator the effect of BIA is ignored and the interface localised contribution to the optical matrix element is disregarded.

We will investigate the energy level positions, spin split of states, and optical matrix elements for the optical transitions cause by light polarized along the growth direction in an InAs/GaSb quantum well with a 10 nm InAs layer and a 10 nm GaSb layer. It is sandwiched by the two 10 nm wide-gap AlSb barrier layers and the two n-type InAs contact layers. We take the material and structure parameters: interband momentum matrix elements, Lattinger parameters, split-off energies in different layers, band offsets at the heterojunctions, BIA- and IH-parameters, etc. the same as in Refs. [11, 12]. We set the donor concentration in each InAs contact layer to $10^{18}\,\mathrm{cm}^{-3}$.

First we will consider the results on the energy level positions of the electron and hole states in the InAs/GaSb quantum well. Then the optical properties will be investigated for the mid-infrared transitions between the states of different subbands of size quantization and different spin orientations. The energy levels in the quantum well with a 10 nm InAs layer and a 10 nm GaSb layer are shown in Fig. 1 in solid curves. The Fermi level in the quantum well is marked by dashed line. All results in Fig. 1 are obtained using our full Hamiltonian. The levels at $\mathbf{k}_{\|}=0$ are assigned by labels $1hh$, $2hh$, and $3hh$ for the first, second, and third heavy-hole-like subbands, respectively, $1e$ and $2e$ for the first and second electron-like subbands. The $1lh$ label is for the states of the first light-hole-like subband. At $\mathbf{k}_{\|} \approx 0.14\ \mathrm{nm}^{-1}$ the $1e$ and $1hh$ subbands anticross and the hybridization gap forms in the in-plane dispersion. We show in Fig. 1, for example, the dispersions for the [10] and [12] directions of quasiparticle in-plane wave vector. The anisotropy of dispersions is weak, however the anisotropy of spin split of levels can be large for different electron-like and hole-like subbands that influences the mixing of electron and hole states with different spins and optical matrix elements due to effects of SIA, BIA, relativistic IH, and non-relativistic IH.

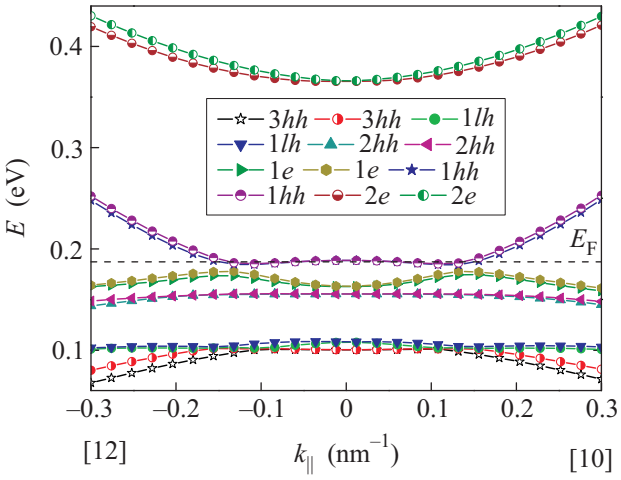

Fig. 1. (Color online) The subband dispersions in the InAs/GaSb quantum well shown in solid curves. The Fermi level is shown in dashed line

The spin split of the $1e$, $2e$, $1hh$, and $2hh$ subband states is presented in Figs. 2 and 3. Just these states participate in the optical transitions ($1e$–$2e$, $1hh$–$2e$, $2hh$–$2e$) near the absorption edge for the incident mid-infrared radiation. In the following consideration in region of small $k_{||}$, the lower dispersion branch of each subband will be assigned with a subscript a and the upper with a subscript b. The spin split for the $1e$ states in Fig. 2 obtained with full Hamiltonian is shown in solid curves for the [10] and [12] directions of in-plane wave vector. On the other hand, dash-dotted curve in this figure has been obtained with neglect BIA and IH. The difference between the values of spin split shown in solid and dash-dotted curves is small for the [10] direction of in-plane wave vector, however it is considerable for the low symmetry [12] direction. The main contribution to this difference comes from the BIA-terms in Hamiltonian. The effect of IH on the spin split of the $1e$ subband states is small. The two peaks of ΔE appear near the $1hh$–$1e$ subband anticrossing points. The results for the spin split of the $2e$ levels obtained using full Hamiltonian are shown in solid curves. The Hamiltonian, where the non-relativistic IH is neglected, has been used to obtain dashed curves. Full IH is disregarded to found the spin split of the $2e$ levels shown in dotted curves. BIA and IH are neglected for the re-

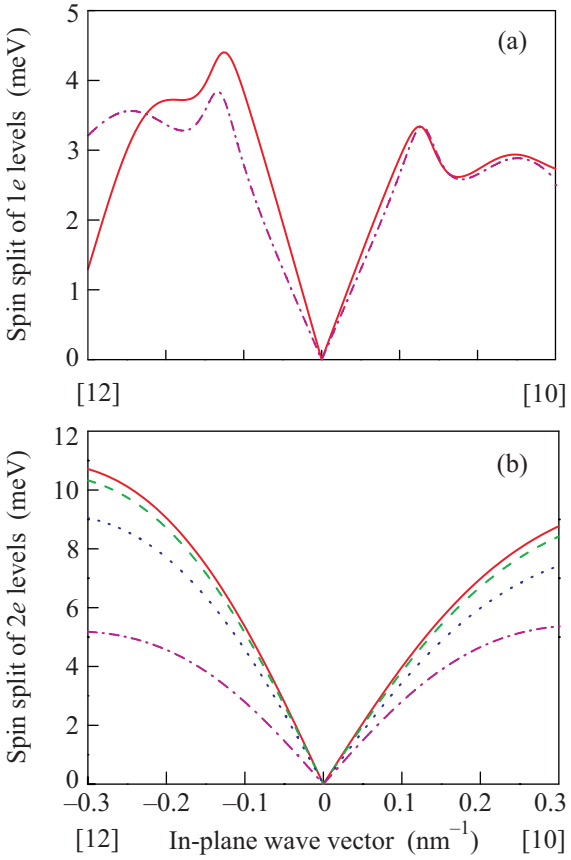

Fig. 2. (Color online) Absolute values of spin split of the $1e$ (a) and $2e$ (b) subband states shown in solid, dashed, dotted, and dash-dotted curves for the different models

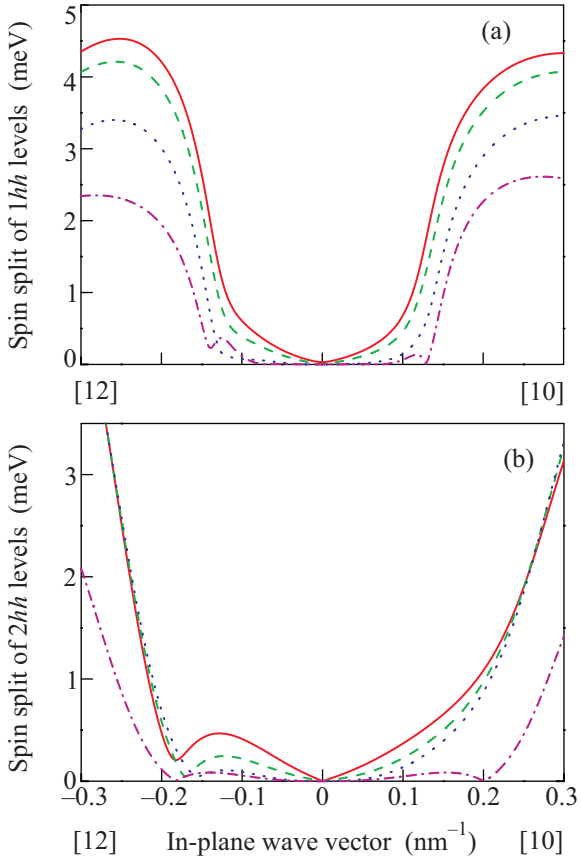

Fig. 3. (Color online) Similar plots as in Fig. 2, but for the spin split of the $1hh$ (a) and $2hh$ (b) subband states

sults represented by dash-dotted curve. The spin split of the $2e$ subband states is mainly due to SIA and BIA. However the effect of IH is also important. The spin split enlarges considerably with the in-plane wave vector increasing and is greater for the [12] direction of the in-plane wave vector than for the [10] direction.

In Fig. 3, the solid, dashed, dotted, and dash-dotted curves correspond to the same models as in the lower panel of Fig. 2. The spin split of the $1hh$, $2hh$, and $1e$ states is much less than that of the $2e$ levels. This is because the effect of BIA on ΔE enlarges with the energy level position increasing due to terms of type $\hat{k}_z B\hat{k}_j$, $\hat{k}_j B\hat{k}_z$, with $j = x$ or y. The dash-dotted curve for the [10] direction of in-plane wave vector, which represents the spin split of the $1hh$ states due to the SIA only, coincides with the horizontal axis at some point near hybridization gap. Then the spin split is zero, because the dispersion curves for the $1hh_a$ and $1hh_b$ states cross and the $1hh_a$ energy level becomes higher than the $1hh_b$ energy level. This means than the spin split states in this case do not mix and do not interact. The effect of warping terms in Hamiltonian results in transformation of the crossing point into the anticrossing point for the [12] direction of the in-plane wave vector. With account of the BIA and IH, the states of the $1hh$ subband with different spins interact and their states hybridize that results in the transformation of level crossing into the level anticrossing.

The BIA and IH contribute considerably to the spin split of the $1hh$ subband both for the [10] and [12] directions in the plane of the quantum well. However, the IH almost does not influence the spin split of the $2hh$ subband states. The mixing and interaction of states with different spins result in a substantial contribution of the spin-flip inter-subband transitions into the total optical transition probability.

We will consider the optical transitions between the states of the $1e$- and $2e$-subbands and the states of the $1hh$- and $2e$-subbands when the initial state in-plane wave vector is along the [10] or [12] direction. Since the states with different spins mix and interact because of BIA and IH, the originally forbidden spin flip $1hh$–$2e$- and $1e$–$2e$-transitions for the $\mathbf{k}_\parallel$ along [10] direction can be essential [1, 13]. However, the nonzero but very small mixing of states with different spins resultant only the warping occurs when the initial state in-plane wave vector is along some low symmetry direction such as [12]. Then the spin-flip transitions can take place even with neglect BIA- and IH-terms, but the intensity of these transitions is small. The combined effect of warping, BIA, and IH leads to considerable enlarge of the intensity of spin-flip transitions. They become much more substantial than those for the high symmetry [10] direction of the initial state in-plane wave vector.

To demonstrate this effect, we show in Fig. 4 the absolute values of normalized optical matrix elements

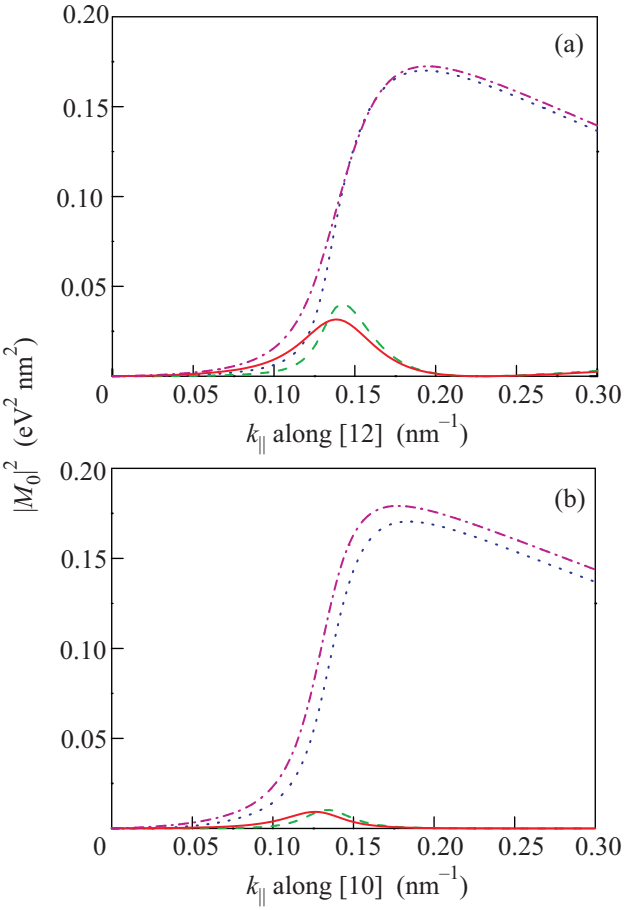

Fig. 4. (Color online) Square of the absolute value of the optical matrix elements for the $1hh$–$2e$-transitions. The solid, dashed, dotted, and dash-dotted curves represent, respectively, $1hh_b$–$2e_a$-, $1hh_a$–$2e_b$-, $1hh_a$–$2e_a$-, and $1hh_b$–$2e_b$-transitions. Light polarization is along the z-axis and $\mathbf{k}_\parallel$ is along the [12] direction and [10] direction

squared $|M_0|^2 \equiv |\hbar M/\sqrt{2m}|^2$ for the $1hh$–$2e$-transitions when $\mathbf{k}_\parallel$ is along the [12] direction or along the [10] direction. The solid, dashed, dotted, and dash-dotted curves are, respectively, for the $1hh_b$–$2e_a$-, $1hh_a$–$2e_b$-, $1hh_a$–$2e_a$-, and $1hh_b$–$2e_b$-transitions. All four types of optical matrix elements are nonzero in each panel of Fig. 4 and the corresponding transitions can contribute into the absorption coefficients. If we neglect BIA- and IH-terms, then the spin-flip transitions for $\mathbf{k}_\parallel$ along [10] direction shown in solid and dashed curves vanish. The main contribution into the absorption coefficients from the spin-flip transitions comes from the region around the hybridization gap. Then the electron and hole states with

different spins are strongly mixed and their wave functions are substantial in the InAs layer and in the GaSb layer of the quantum well. The optical matrix elements for the spin-conserved $1hh$–$2e$-transitions are considerable when the states of the $1hh$ subband are hybridized with the $1e$ subband states or become electron-like after the anticrossing with the $1e$-levels.

Similar plots as in Fig. 4, but for the $1e$–$2e$-transitions, are shown in Fig. 5. The solid, dashed, dotted, and dash-dotted curves are, respectively, for the $1e_b$–$2e_a$-, $1e_a$–$2e_b$-, $1e_a$–$2e_a$-, and $1e_b$–$2e_b$-transitions. Contrary to the $1hh$–$2e$-transitions, the values of $|M_0|^2$ for the $1e$–$2e$-transitions are considerable at sufficiently small values of $\mathbf{k}_\parallel$ along [12] direction and along the [10] direction where the $1e$ subband states are the electron-like. The spin-flip transitions shown in solid and dashed curves are much more essential for the [12] direction of the initial state in-plane wave vector than for the [10] direction for all considered optical matrix elements.

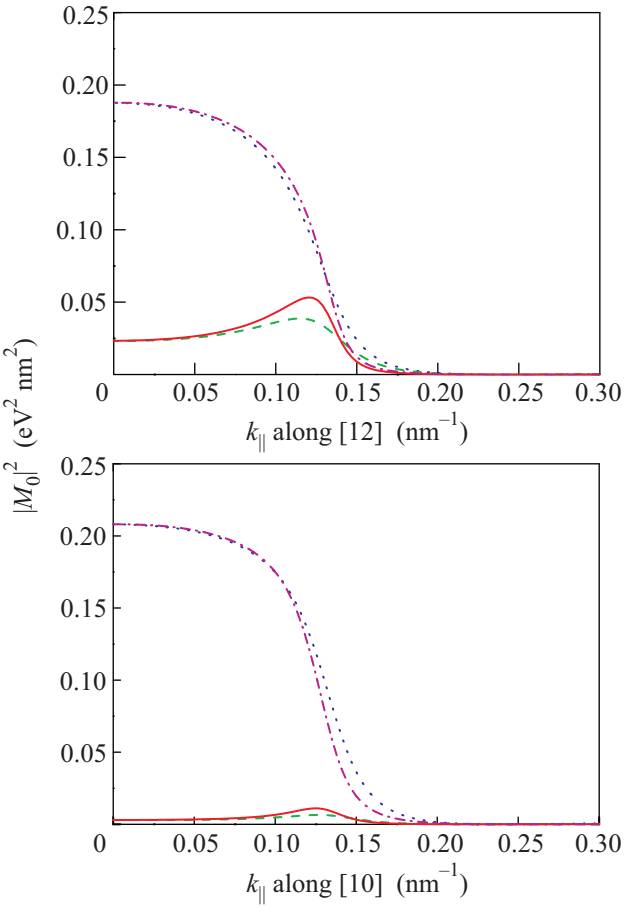

Fig. 5. (Color online) Square of the absolute value of the optical matrix elements for the $1e$–$2e$-transitions. The solid, dashed, dotted, and dash-dotted curves represent, respectively, $1e_b$–$2e_a$-, $1e_a$–$2e_b$-, $1e_a$–$2e_a$-, and $1e_b$–$2e_b$-transitions. Light polarization is along the z-axis and $\mathbf{k}_\parallel$ is along the [12] direction and [10] direction

In summary, we have considered theoretically the effect of warping and symmetry breaking on spin split of levels in asymmetrical quantum wells grown along the [001] direction as well as on optical matrix elements for the transitions between the states of different subbands caused by light linearly polarized along the growth direction. The considered InAs/GaSb quantum wells sandwiched by the two AlSb barrier layers have the two-dimensional hybridized electron-hole states from which the optical transitions in the infrared photon energy range can occur. The warping terms in Hamiltonian, BIA, relativistic and non-relativistic IH mix the spin-up and spin-down states of different subbands, that influences the dispersion curves, spin split of levels and optical matrix elements. We have found a substantial influence of relativistic and non-relativistic IH on the spin split of the heavy-hole levels. The warping, BIA- and IH-transform the subband crossing points into the anticrossing points. Due to the combined effect of warping and symmetry breaking, the intensity of spin-flip optical transitions are much greater for low symmetry directions of $\mathbf{k}_\parallel$ then for high symmetry direction [10] ([01]).

This work was supported by the Russian Foundation for Basic Research under grants # 07-02-00680-a and 03-02-16788-a and by Royal Swedish Academy of Sciences for cooperation between Sweden and former Soviet Union.

1. I. Semenikhin, A. Zakharova, K. Nilsson, and K. A. Chao, Phys. Rev. B **76**, 035335 (2007).
2. M. Altarelli, Phys. Rev. B **28**, 842 (1983).
3. J. Luo, H. Munekata, F.F. Fang, and P. J. Stiles, Phys. Rev. B **38**, 10142 (1988); Phys. Rev. B **41**, 7685 (1990).
4. R. Q. Yang, Superlatticies Microstrt. **17**, 77 (1995).
5. J. C. Chiang, S. F. Tsay, Z. M. Chau, and I. Lo, Phys. Rev. Lett. **77**, 2053 (1996).
6. M. J. Yang, C. H. Yang, B. R. Bennett, and B. V. Shanabrook, Phys. Rev. Lett. **78**, 4613 (1997).
7. L. J. Cooper, N. K. Patel, V. Drouot et al., Phys. Rev. B **57**, 11915 (1998).
8. L. W. Wang, S. H. Wei, T. Mattila et al., Phys. Rev. B **60**, 5590 (1999).
9. R. Magri, L. W. Wang, A. Zunger et al., Phys. Rev. B **61**, 10235 (2000).
10. E. Halvorsen, Y. Galperin, and K. A. Chao, Phys. Rev. B **61**, 16743 (2000).
11. X. Cartoixa, D. Z.-Y. Ting, and T. C. McGill, Phys. Rev. B **68**, 235319 (2003).
12. A. Zakharova, S. T. Yen, and K. A. Chao, Phys. Rev. B **66**, 85312 (2002).

13. I. Semenikhin, A. Zakharova, and K. A. Chao, Phys. Rev. B **77**, 113307 (2008).
14. A. Zakharova, I. Semenikhin, and K. A. Chao, Semicond. Sci. Technol. **23**, 125044 (2008).
15. I. Vurgaftman and J. R. Meyer, Phys. Rev. B **70**, 115320 (2004).
16. I. V. Tokatly and E. Yu. Sherman, Phys. Rev. B **82**, 115320 (2010).
17. M. G. Burt, J. Phys.: Condens. Matter **4**, 6651 (1992).
18. B. A. Foreman, Phys. Rev. B **56**, R12748 (1997).
19. D. Gershoni, C. H. Henry, and G. A. Baraff, IEEE J. Quant. Electronics **29**, 2433 (1993).